

DYNAMOMETER ANALYSIS PLOTS IMPROVE ABILITY TO TROUBLESHOOT AND ANALYZE PROBLEMS

A. L. Podio, University of Texas
J. N. McCoy, O. Lynn Rowlan and Dieter Becker
Echometer Company

ABSTRACT

Dynamometer Analysis Plots allow the display of various parameters; both acquired and calculated, during a complete pumping unit stroke. At a user-specified time frequency, the polished rod load, polished acceleration, electrical motor power, and current data are acquired during a dynamometer survey at a sucker rod lift well. Using the descriptive well information and pumping unit geometry many other parameters are calculated, such as: pump load, polished rod position, polished rod velocity, pump plunger position, pump plunger velocity, existing mechanical and electrical net gearbox torque, instantaneous SPM, and motor RPM. These calculated and acquired dynamometer parameters can be plotted, in pairs, in any combination versus any of four horizontal axis parameters; polished rod position, plunger position, elapsed time, or crank angle. Analysis of operational problems can be aided through the ability to graphically compare the various acquired and calculated data values. Frequently the standard plots of load vs. position or vs. time displayed by analysis software programs are not sufficient to trouble shoot and analyze a sucker rod lift problem. Providing a user the graphic capability to easily select and compare the different acquired and calculated parameters for a selected individual stroke, leads to better understanding and analysis of the sucker rod lift producing conditions.

INTRODUCTION

The Dynamometer Analysis Plots allow plotting many different graphs that are not the standard type of plots displayed by existing software for the analysis of sucker rod pumping systems. The plots can be displayed for an individual stroke within a series of data for multiple pump strokes. A vertical indicator marker can be scrolled through the data displayed on the plot and the numeric values from the displayed curves at the marker are presented in text boxes below the horizontal axis for quantitative analysis. The parameters that are available for plotting purposes are:

- polished rod load
- pump load
- motor current (Amps)
- motor power (KW)
- polished rod position
- polished rod velocity
- polished rod acceleration
- filtered polished rod acceleration
- plunger position
- plunger velocity
- mechanical net gearbox torque (existing)
- mechanical net gearbox torque (balanced)
- power net gearbox torque (existing)
- power net gearbox torque (balanced)
- rod torque (existing)
- counterbalance torque (existing)
- instantaneous SPM
- torque factor
- motor RPM.

These calculated and acquired dynamometer parameters can be plotted in any combination of pairs versus any one of the four horizontal axis parameters:

- polished rod position
- plunger position
- elapsed time
- crankangle.

Graphic comparative displays of different types of data can aid in the analysis of a sucker rod lift system, but usually in most software programs the plots are fixed and optional display of data is not available. By using these analysis plots, 1530 unique plots can be generated by selecting from a possible combination of 20 parameters for vertical right axis, 19 parameters for vertical left axis, and four possible parameters for the horizontal axis. Analysis of operational problems of the sucker rod lift pumping system can be enhanced through the ability to compare the various acquired and calculated data values on an individual stroke basis.

Through the use of high performance digital data acquisition systems a complete analysis of a sucker rod lift pumping system can be performed. The data acquisition system consists of a laptop computer, an analog to digital converter, and a load cell with accelerometer, and motor current/power sensors. The load cell uses a strain gauge to measure the load on the polished rod. The load cell can either be of the horseshoe type, which is positioned on the polished rod between the carrier bar and the polished rod clamp, or of a special design that is easily clamped directly onto the polished rod. The electrical motor current/power sensors are connected to the switch box, thus the power and current input into the motor are acquired. The signals from the load cell and sensors are sent to the (A/D) converter for conditioning and digitizing at a user-specified sampling frequency. The digital data is then routed to the computer where the signals can be processed and displayed by software and simultaneous measurement of dynamic parameters (polished rod load, polished rod acceleration, motor power, and motor Amps data) may be monitored and recorded. The operator can acquire at least one minute of polished rod load, acceleration, and motor current and power data. Numerical integration of the acceleration signal versus time is used to calculate the velocity and the position of the polished rod. This polished rod load and position data is typically processed to plot a surface dynamometer card and calculate a pump dynamometer.

The surface dynamometer and pump dynamometer card plots are the most common plots used to analyze the operation of a sucker rod pumping system. The surface dynamometer card is the plot of measured or predicted polished rod load at the various positions throughout a complete stroke. The pump dynamometer card is a plot of the calculated load at various positions of pump stroke and represents the load the pump applies to the bottom of the rod string. Identifying how the pump is performing and analyzing downhole problems is one of the primary uses of the pump dynamometer card. Analysis of the surface and pump dynamometer card do not always allow complete performance diagnosis of the sucker rod lift system and occasionally additional display of the acquired and calculated data would be helpful.

The following sections describe special analysis plots of operational data and show how the understanding of the performance of the equipment can be aided through the ability to visually compare various acquired and calculated data values.

POLISHED ROD AND PLUNGER POSITION VERSUS TIME

The polished rod position and plunger position versus time plots aid in the understanding of the movement of the pump plunger relative to the polished rod position. Rod stretch occurs when the rods pick up the differential fluid load on the plunger during the upstroke. Rods un-stretch by releasing or transferring of the fluid load from the rods back to the tubing during the beginning of the down stroke. Unanchored tubing stretch occurs during the transfer of fluid load from the rods to the tubing during the early part of the down stroke. Tubing un-stretch occurs when the fluid load is transferred from the tubing to the rods.

For one complete stroke the positions of both the polished rod and the pump plunger are shown by the two curves in **Fig. 1**. This figure is an excellent example of the effect of rod stretch on plunger motion for a well with anchored tubing. During the 8.97 seconds of elapsed time for one stroke, the surface stroke has a general sinusoidal shape with a maximum stroke length, S , of 86 inches, while the magnitude of the plunger stroke, S_p , is 59 inches. Starting at the beginning of the upstroke, point **A**, the polished rod moves upward in a sinusoidal fashion with respect to time. The pump plunger remains stationary while the rods gradually stretch, until the fluid load, force from the differential pressure across the plunger, is transferred from the tubing (standing valve) to the stretched rods (traveling valve). At point **B**, the rods have stretched enough to apply a force equal to the fluid load on the plunger and the plunger begins to move upward. The plunger does not move relative to the anchored tubing for the time period from point **A** to point **B** and the plunger has zero velocity (displacement/time) during this time period, if there were fluid slippage between the plunger and the pump barrel, then the plunger would move relative to the anchored tubing. During the rest of the upstroke, the rod stretch remains approximately constant and the plunger and polished rod move together. Point **C** is at the beginning of the down stroke, the plunger again remains stationary, while the rod stretch decreases. The fluid load at point **C** is beginning to be transferred from the rods and plunger back to the closed standing valve attached to the anchored tubing string. At point **D**, where the stretch on the rods due to the fluid load becomes zero, the plunger is completely unloaded and again both plunger and polished rod move together on the down stroke. At the end of the stroke, 8.97 seconds of time have elapsed, the stroke is complete and the process is repeated for each additional stroke. A flat line for plunger position from points **A** to **B** and

from points C to D is an indication that the traveling and standing valve are not leaking, the tubing anchor is holding, and very little fluid slippage through the clearance between the plunger and barrel is occurring. **Fig. 2** is an example of a pump with a leaking traveling valve in a well with anchored tubing. The plunger motion for the time period from point A to point B is much larger when compared with the same interval in **Fig. 1**, indicating that the plunger has to move a greater distance before the pressure in the barrel decreases to the point where the standing valve opens and fluid enters the barrel of the pump. Due to the lower difference in pressure between the barrel and the bottom of the tubing there is less rod stretch and the motion of the plunger tends to follow more closely the motion of the polished rod. This is verified by the valve check test shown in **Fig. 3** that shows that the traveling valve is leaking at a rate of about 80 Bbls/day

Fig. 4 is an example of the effect of tubing stretch on rod stretch and plunger motion for a well with un-anchored tubing. Note the similarity with **Fig. 2** for a TV leak. The similar shape of the plunger motion of un-anchored tubing and a leaky traveling valve shows that it is important to know exactly what hardware has been installed in the well, so that the diagnostic data may be interpreted correctly. During the 12.45 seconds of elapsed time for one stroke, the surface stroke has a general sinusoidal shape with a maximum stroke length, S , of 100 inches, while the maximum plunger stroke, S_p , is 69.6 inches. Starting at the beginning of the upstroke, point A, the polished rod moves upward in a sinusoidal fashion with respect to time. Both the tubing and plunger are moving from point A to point B, the tubing shortens as the rods gradually stretch so that there is little relative motion between the barrel and the plunger. At point B, the rods have stretched enough to apply a force equal to the fluid load on the plunger and the plunger begins to move upward relative to the tubing. The maximum plunger stroke occurs at point C, but no pump displacement occurs from point C to point D as the fluid load is transferred from the rods and plunger back to the closed standing valve attached to the un-anchored tubing string. The vertical distance between points C and D is the plunger stroke that is lost due to tubing movement. The effective plunger stroke is the vertical height of point D, where the standing valve closes holding the fluid in the tubing. The rod stretch due to the fluid load becomes equal to zero at point D, where the fluid load on the plunger is zero and both plunger and polished rod move together during the rest of the down stroke. At the end of the stroke, 12.45 seconds of time have elapsed, the stroke is complete and the process is repeated for each additional stroke. Tubing movement due to a slipping anchor or un-anchored tubing is often best diagnosed through inspection of the plot of polished rod and plunger position.

DIAGNOSING PUMPING SYSTEM PROBLEMS

Fig. 5 shows a plot of the polished rod and plunger position vs. time where the motions of the top and bottom of the rod string are essentially identical in time. The lack of any appreciable difference is caused by the absence of any rod stretch due to the lack of fluid load on the plunger. This could be caused by a permanently open traveling valve, a totally worn plunger or by a rod failure in the vicinity of the pull rod. In this case the rods had parted just above the pump. The small difference in position at points A and B are due to the acceleration effect at the beginning of the upstroke and the start of the downstroke that cause a small elongation of the rod string.

Fig. 6 shows that in this well the plot of plunger load versus time follows an erratic pattern. At the beginning of the plunger stroke during about 2.4 seconds the load remains constant then increases suddenly as the plunger continues rising, then the load decreases even before the plunger starts moving down. The rapid increase in load is caused by the traveling valve closing suddenly during the middle of the upstroke and then opening before the top of the stroke is reached. This is also reflected in the surface dynamometer card, shown in **Fig. 7**, that shows a sudden increase in load halfway on the upstroke. This effect could be caused by debris preventing the valve from operating properly. However in this well the effect is due to a case of “flumping” (intermittently flowing and pumping) due to a very high gas production (635 MSCF/day) and gaseous liquid column and an inefficient downhole gas separator that allows large volumes of gas to flow through the pump.

Fig. 8 shows a dynamometer card for another well (well A), which is very similar to the dynamometer in **Fig. 7**. However in this well the fluid level was near the pump intake and gas production was not excessive. The dynamometer shown in **Fig. 8** occurred intermittently about 30 % of the time. **Fig. 9** shows the corresponding plot of polished rod and plunger position vs. time, which shows that at the beginning of the upstroke the plunger follows the motion of the polished rod, indicating that the traveling valve is open, then the plunger stops shortly (where the dashed line is located) for about 0.5 seconds, and then the plunger rises almost normally. **Fig. 10** shows the same plot of plunger and polished rod position vs. time during a normal stroke with a full pump. The intermittent malfunction of the traveling valve was later attributed to “gunk in the pump” caused by the misuse of chemicals.

Fig. 11 shows a set of unusually shaped polished rod and pump dynamometer cards for Well B, that also show large peak polished rod load in relation to a rod weight in fluid of about 16,000 Lbs. Using the diagnostic plots and looking at **Fig.**

12 during the first 2.5 seconds it is clearly seen that the plunger seems to move in an opposite direction to that of the polished rod. **Fig. 13** shows a plot of polished rod load and position vs. time, that for practical purposes indicates the polished rod load and position follow the same (near sinusoidal) pattern indicating that the load is directly proportional to the polished rod position. Based on Figures 12 and 13 one may conclude that the plunger or the rods are probably stuck at least for part of the stroke. **Fig. 14** further supports this conclusion, which is a plot of polished rod load vs. polished rod position for the upstroke. The best-fit line through the data has a slope of 170 Lbs/inch, which closely matches the rod string elastic constant for the rod string of 175 Lbs/inch (API rod 86 for a rod length of 8100 feet).

Fig. 15 shows the surface and pump dynamometer cards, for a well with fiberglass sucker rods that exhibit unusual characteristics. On the surface card there is a sudden drop in load (point A) during the upstroke and a sudden increase in load at point B near the top of the stroke. Also the pump dynamometer shows high frequency oscillations of the load during most of the stroke. These unusual features can be explained by looking at **Fig. 16** where the polished rod load and the plunger position are plotted as a function of time. The plunger motion is downwards from time zero to 0.2 seconds and the plunger position remains at zero between 0.2 and 0.5 seconds indicating that the pump has tagged bottom. The red line on the plunger position shows where the plunger was at the very beginning of the upstroke at zero position (time where the tag occurred), the red line on the polished rod load curve is where the tag resulted in a 1400 lb drop in polished rod load. The jump in load occurring at about 1.5 seconds of time (red arrow) is caused by the tag being reflected from the surface and traveling round trip back to the surface. The elapsed time axis is for the time reference of the surface dynamometer data, it takes around 0.3-0.4 seconds for the stress wave at the pump to travel to the surface. This mechanism explains the high frequency “noise” observed on the pump dynamometer and seen on **Fig. 17** where the pump load and plunger position are plotted vs. time. The observed signals correspond to multiples (indicated by arrows) of the stress wave generated by tagging bottom as it repeatedly travels from the bottom to the top of the rod string and back to the pump. The uniform spacing of the signals at about 0.7 seconds correspond to the two way travel time of the stress wave in the rod string. Note that the amplitude of the impact corresponds to about 4000 Lbs (peak to peak), which will eventually cause damage to the rods.

MECHANICAL AND POWER NET GEARBOX TORQUE

Both dynamometer data acquired using a load cell at the polished rod and power data acquired using power probes connected to the panel can be used to determine instantaneous net gearbox torque. The net gearbox torque is determined by two completely independent methods; where one method uses measured motor power, motor and drive efficiencies and the pumping unit speed to determine the net gearbox torque and the other method uses the measured surface dynamometer card and calculated torque factors together with counterbalance moments from the crank and weights to determine the net gearbox torque. **Fig. 18** compares the measured power provided to the motor to the calculated net mechanical gearbox torque, showing that the two independently determined curves are directly proportional. **Eq. 1** is used to calculate net torque at the gearbox during a pump stroke from the measured power data input into the motor.³

$$T_N = 84.5 \times kW \times \text{Eff} / (\text{SPM} \times \text{SV}) \quad (1)$$

The method defined by standard API Spec 11E is used to determine the net mechanical gearbox torque. The torque due to net well load at a given crank position is computed from the torque factor at that position multiplied by the corresponding net well load.

Net well load is:

$$W_N = \text{net well load} = (W - \text{SU}) \quad (2)$$

And SU is the structural unbalance of the surface unit.

Torque due to net well load is:

$$T_{WN} = \text{TF} \times W_N \quad (3)$$

Torque due to crank and counterweights is:

$$T_{CN} = \text{Me} \times \sin(\theta + \tau) \quad (4)$$

And Me is the existing counterbalance moment.

Fig. 19 displays the torque due the net well load compared to the torque due to the cranks and counterweights. The arrows represent net gearbox torque, which is the difference between the torque due to net well load and the torque due to the counterbalance moment of the crank and counterweights. This same net gearbox torque, T_N , about the crankshaft is

also shown in **Fig. 18** and is given by the following equation:

$$T_N = TF \times W_N - Me \times \text{sine}(\theta + \tau) \quad (5)$$

The existing net gearbox torque, T_N , is calculated using **Eq. 5** at each crank angle corresponding to a measured load using the API pumping unit dimensions to calculate the torque factor, and the crank and master/auxiliary weight specifications. The best method to balance torque loading on a pumping unit gearbox is to use both power and mechanical methods at the same time to determine the existing net gearbox torque. When viewing the plot of net gearbox torque calculated from measured power overlain on the net gearbox torque calculated from polished rod load and torque factors, it is a simple matter to visually examine the plots and look for discrepancies. These discrepancies usually are an indication of inaccurate descriptive pumping system information in the well file data.

INSTANTANEOUS STROKE PER MINUTE

The instantaneous stroke per minute, SPM, is determined from the change in crank angle between two consecutive polished rod positions. At a user specified sampling frequency the polished rod acceleration is monitored and recorded. The polished rod acceleration data is integrated twice to obtain the polished rod position. The API pumping unit dimensions are used with the polished rod position to determine the corresponding crank angles. The instantaneous SPM shown in **Fig. 20** is equal to the change in crank angle between two consecutive polished rod position data points at the specified sampling frequency (N_{freq}) when compared to the 360 degrees of crank angle rotation in one stroke. The instantaneous SPM (**ISMP**) is calculated by using the following equation:

$$\text{ISMP} = N_{\text{freq}} \times (\theta_{i+1} - \theta_i) / 6 \quad (6)$$

Fig. 20 shows the instantaneous stroke per minute compared to the measured motor power. The arrows on the plot show the broad relationship between motor power and speed, where an increase of the measured power into the motor corresponds to a decrease of the instantaneous SPM. The region of the plot enclosed in the circle shows small spikes of increased measured power corresponding to small decreasing spikes in the instantaneous SPM. The NEMA D motor on this well is well suited to manage cyclic loads experienced during a pumping cycle, under increasing load a property of NEMA D motors is to slow down or slip. The comparison of the two curves on **Fig. 20** clearly shows this property of motors operating under cyclic loading, where the speed of the pumping system changes in inverse proportion to the change in power.

ROTAFLEX POLISHED ROD LOAD VERSUS INPUT MOTOR POWER

The RotaFlex is a mechanically driven long-stroke pumping unit. Usually an electric motor drives the gearbox that is directly connected to a sprocket that drives a long chain at a relatively constant speed. Using a sliding linkage mechanism one of the links of the chain moves the weight box at a relatively constant vertical speed during most of the upstroke and the downstroke. The weight box load balances the polished rod load through a simple pulley connection, where the weight box is connected to one end of a long belt that runs over a drum and the other end of the long belt is connected to the polished rod carrier bar. As the chain link comes in contact with the upper sprocket and the lower sprocket, the link begins to travel at a slower vertical speed until it reverses direction and gradually increases vertical speed until the link is again moving at nearly a constant vertical velocity. **Fig. 21** displays this motion (polished rod position, velocity, and acceleration) of the RotaFlex pumping unit for one stroke. At the top and bottom of the stroke a rapid deceleration and acceleration can be seen to occur, that results in a change of positive to negative vertical velocity of the weight box and polished rod.

Fig. 22 is a plot of polished rod load and motor power vs. time for a complete stroke of the unit. During the upstroke (from 0 to 9 seconds) the weight box and the power input into the motor lift the polished rod load. When the polished rod load increases then almost instantaneously the power increases to continue lifting the polished rod load at nearly a constant velocity. On the downstroke the polished rod load and the power input into the motor lift the weight box. When the polished rod load decreases then almost instantaneously the power increases to continue lifting the weight box at nearly a constant velocity. On the upstroke both power and polished rod load have similarly shaped curves, while on the downstroke the power curve and the polished rod load curve are effectively mirror images. On the upstroke if the polished rod load increases, then the power increases; while on the downstroke the opposite occurs if the polished rod load increases, then the power decreases.

CONCLUSION

Technology derived from computer software is continually evolving and is improving the ability of the operator to better understand and analyze the operation of the sucker rod lift equipment. The advent of portable computers and software has made analysis and acquisition of dynamometer data easier, faster, and more accurate. Use of a portable system permits further in-depth analysis of the sucker rod pumping system at the well site. Analysis of operational problems of the sucker rod lift pumping system can be aided through the ability to compare the various acquired and calculated data values by graphing various combinations of the parameters. Analysis of the surface and pump dynamometer card do not always allow complete performance diagnostics of the sucker rod lift system and the display of additional acquired and calculated data can be helpful in analyzing sucker rod lift systems.

REFERENCES

1. McCoy, J.N., Becker, Dieter, Podio, A.L., and Drake, B., "Improved Analysis of Acoustic Liquid Level Depth Measurements Using Dual Channel Analog/Digital Strip Chart Recorder" presented at the Southwestern Petroleum Short Course, Lubbock, Texas, 1997.
2. McCoy, J.N., Podio, A.L. and Huddleston, K.L.: "Analyzing Well Performance XV," presented at the 1987 Artificial Lift Workshop, Houston, TX, Apr. 22-24.
3. McCoy, J. N., R. E. Ott, A. L. Podio, Forrest Collier and Dieter Becker, "Beam Pump Balancing Based on Motor Power Utilization," SPE 29533 presented at the SPE Production Operations Symposium, Oklahoma City, OK. April 2-4, 1995.

NOMENCLATURE

S	= Surface Stroke Length
Sp	= Plunger Stroke Length
W	= Well load at a specific crank angle
SU	= Structural unbalance of the pumping unit (either plus or minus value)
TF	= Torque factor
M	= Existing counterbalance moment of the crank and counter weights
θ	= Crank angle
τ	= Crank phase angle.
Me	= Existing counterbalance moment of the crank and counter weights
Mer	= Crank counterbalance moment
KW	= Instantaneous motor power
Eff	= Motor/Belts Efficiency
ISPM	= Instantaneous Strokes per Minute
SV	= Speed Variation of the Motor
N <small>freq</small>	= Data Acquisition Sampling Frequency

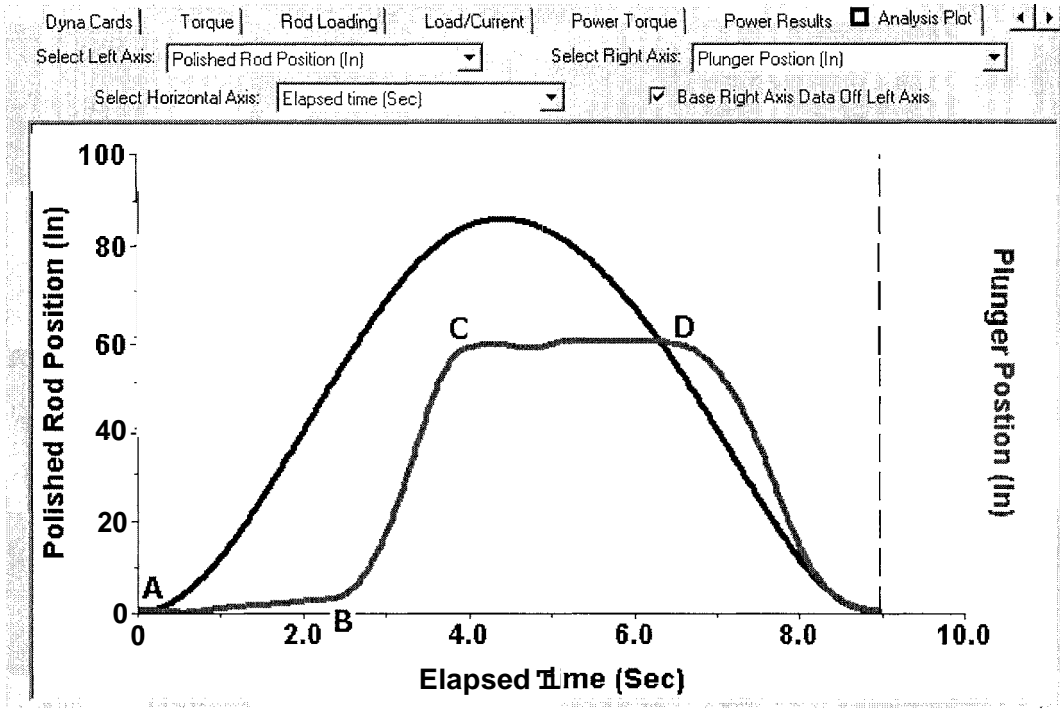


Figure 1 – Polished Rod and Plunger Position vs. Elapsed Time, Anchored Tubing Normal Operation

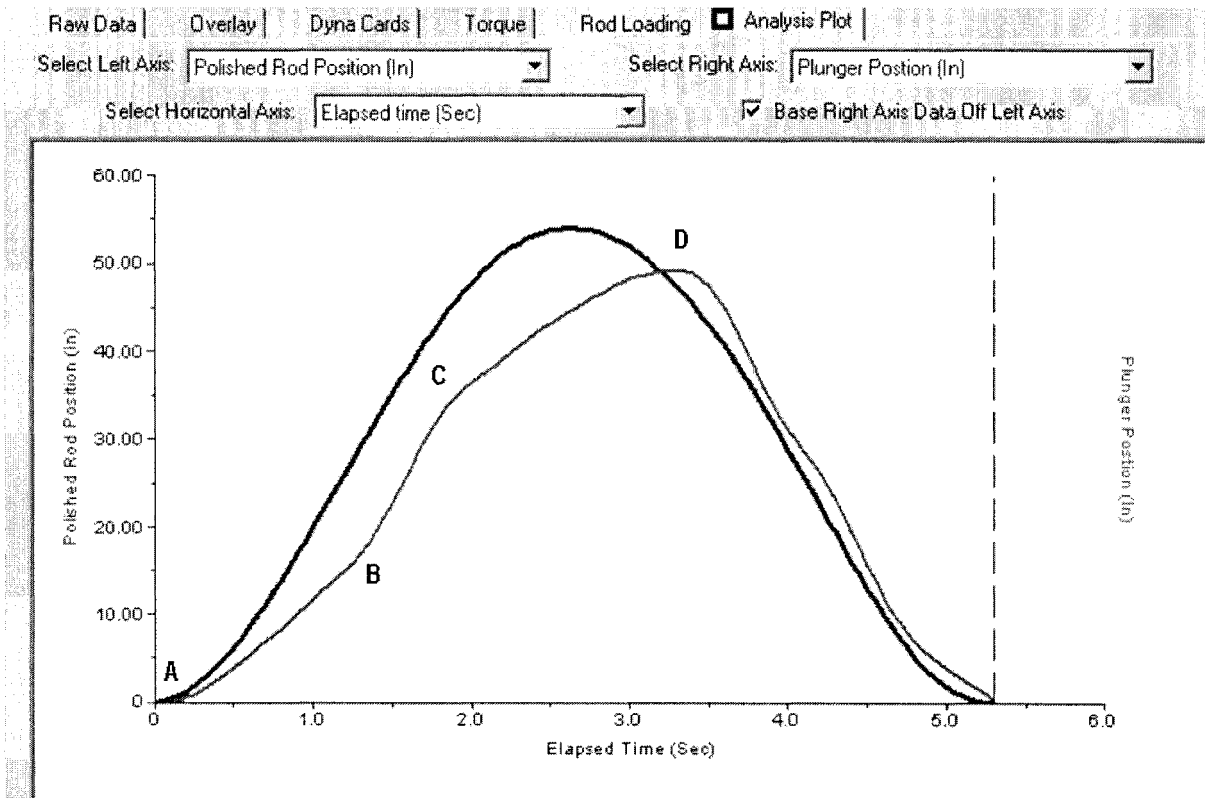


Figure 2 – Same as Figure 1 with Anchored Tubing Except for Leaking Traveling Valve

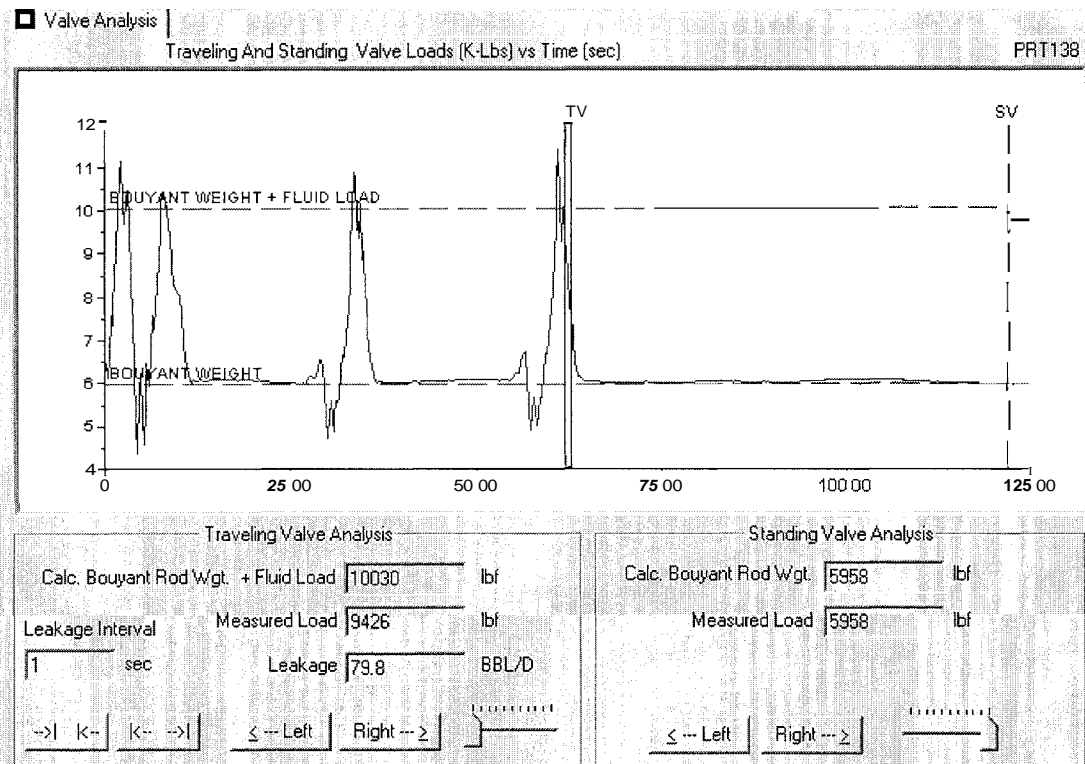


Figure 3 - Valve Check for Well in Figure 2

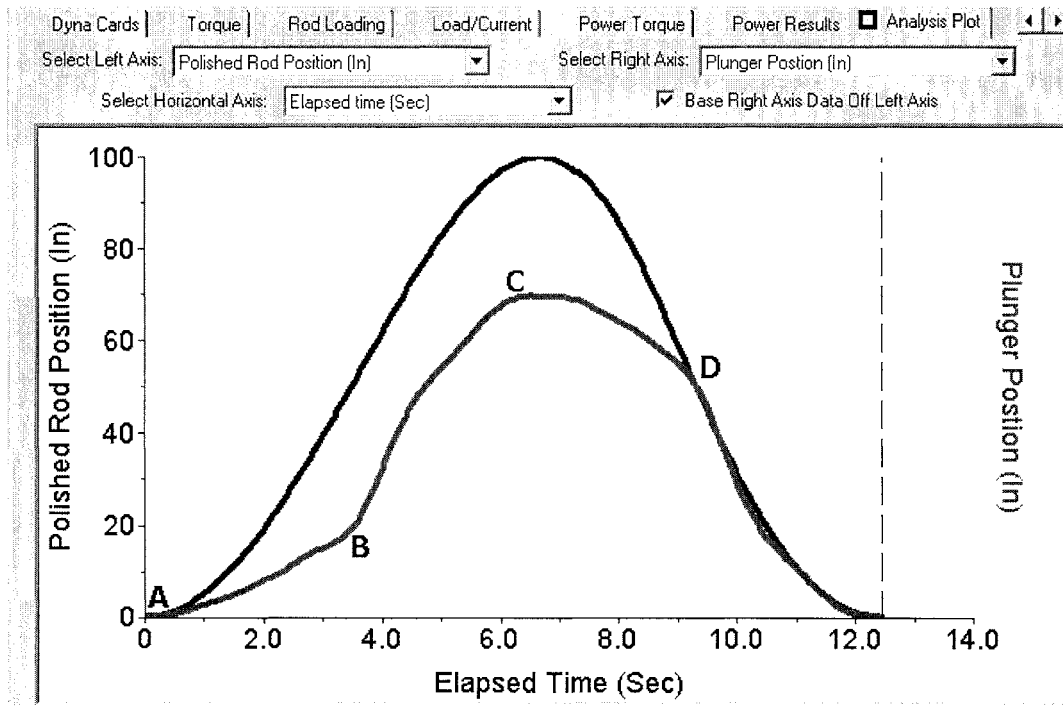


Figure 4 – Polished Rod and Plunger Position Versus Elapsed Time for Un-Anchored Tubing

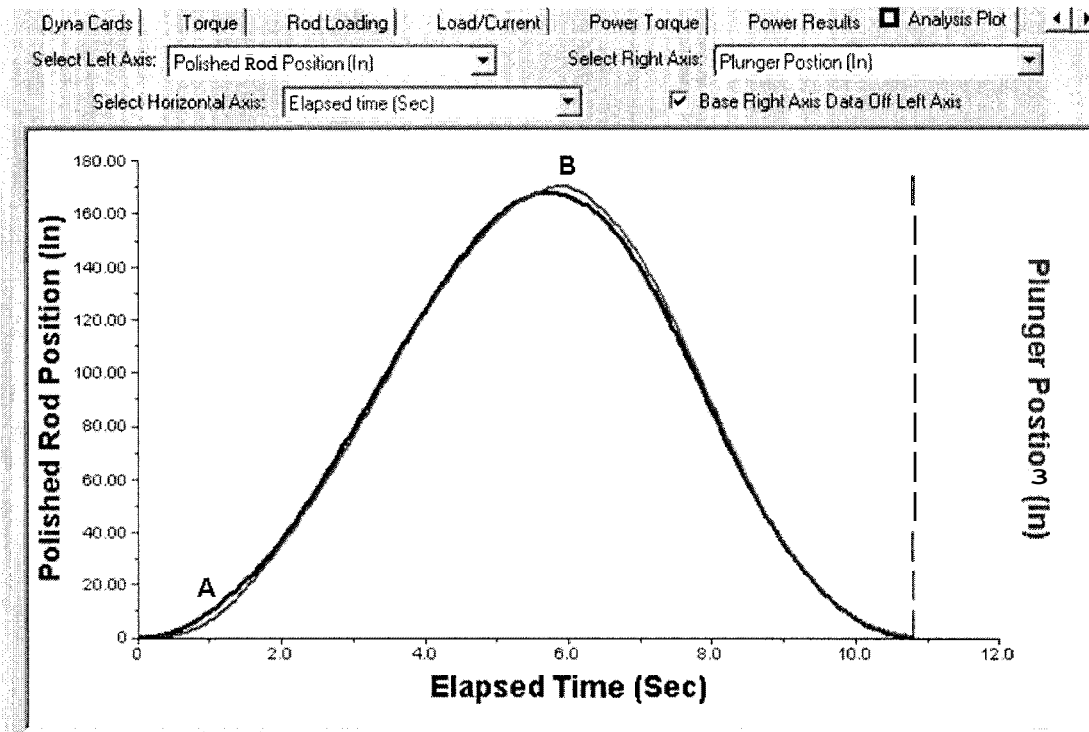


Figure 5 – Polished Rod and Plunger Position Versus Elapsed Time for Parted Rods at Pump

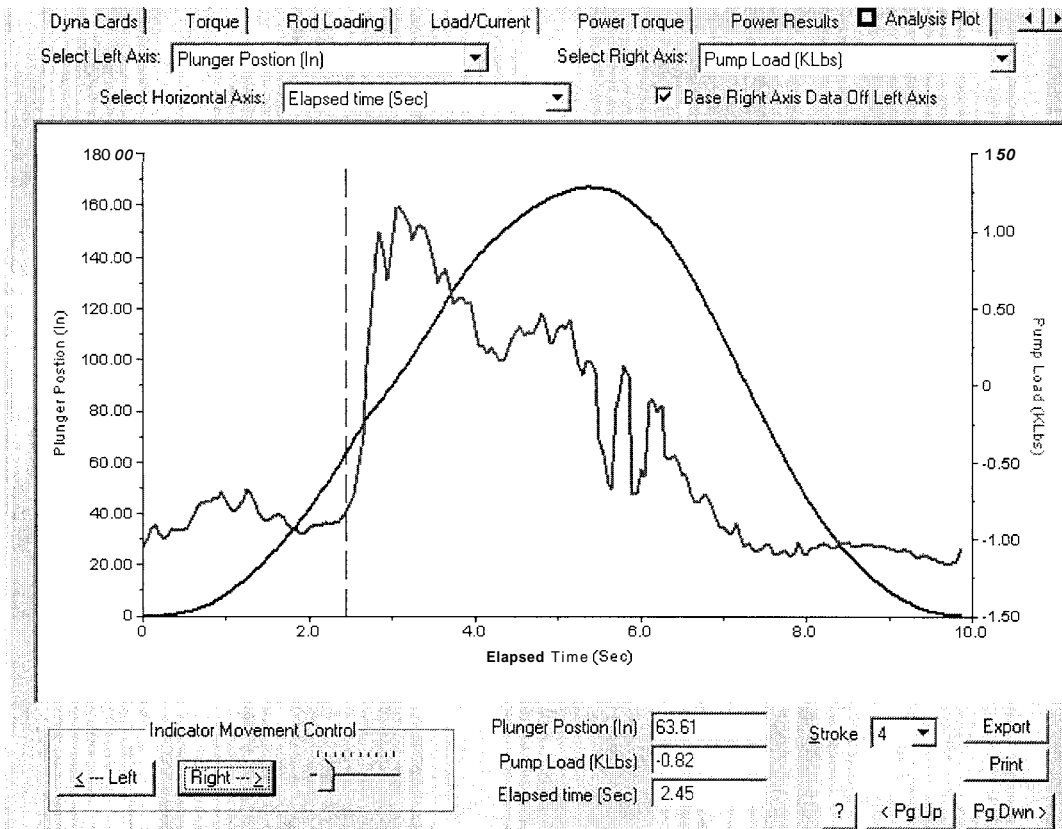


Figure 6 - Pump Load and Plunger Position vs Time for Delayed Traveling Valve Closure

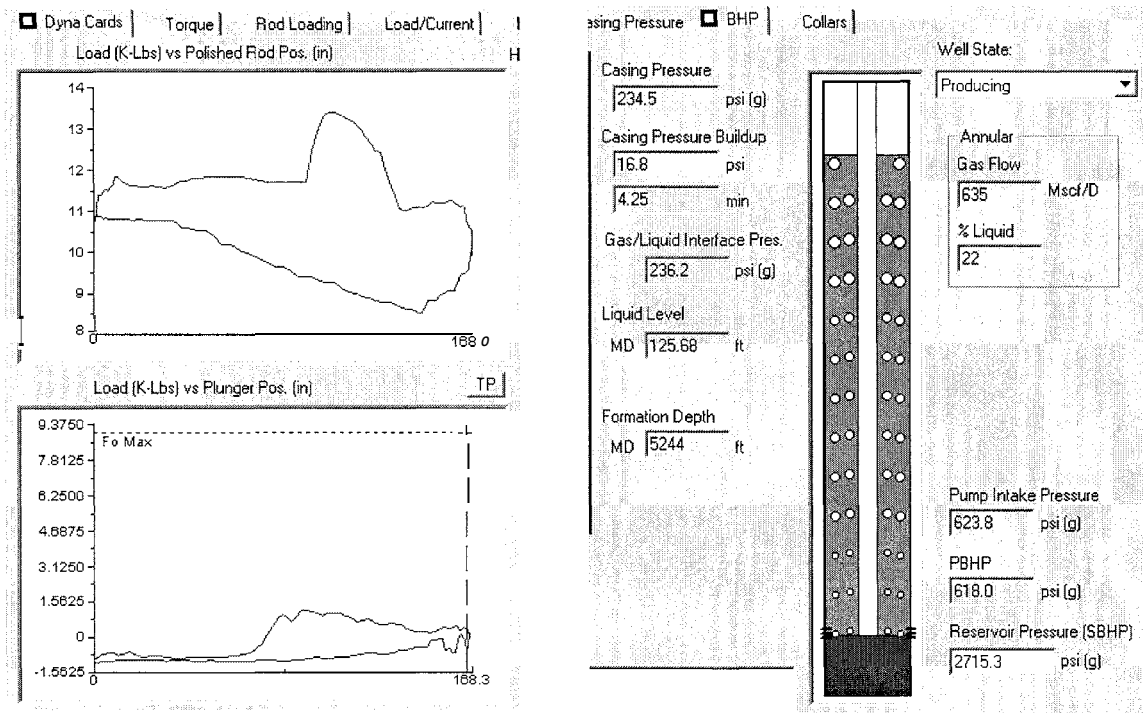


Figure 7 - Polished Rod and Pump Dynamometer Cards for Delayed Traveling Valve Closure

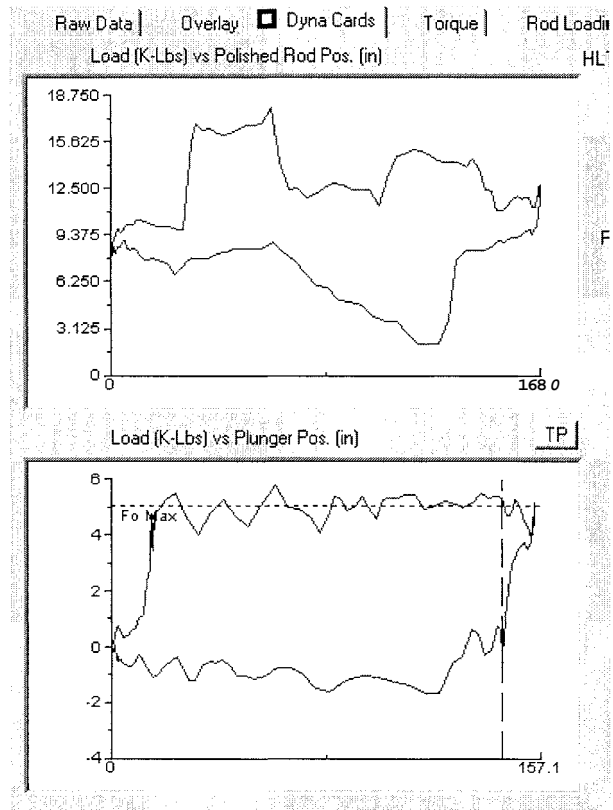


Figure 8 - Surface and Pump Dynamometers for Well A

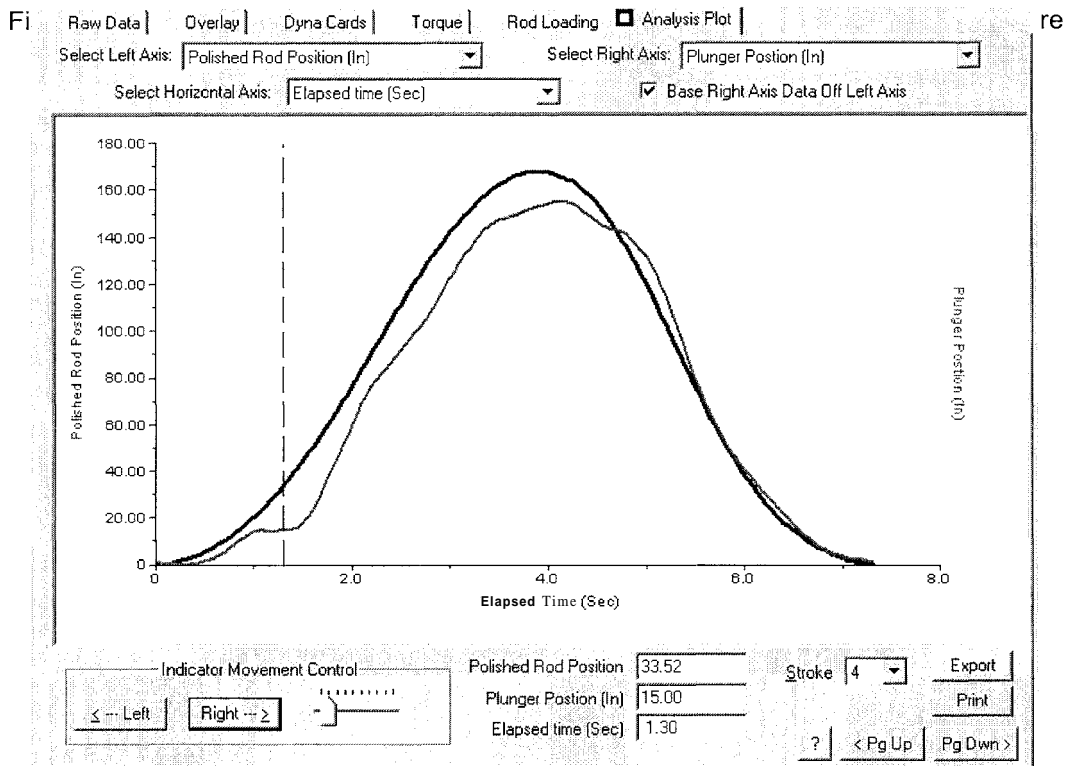


Figure 9 – Polished Rod and Plunger Position vs. Time for Well A (Gunk in Pump)

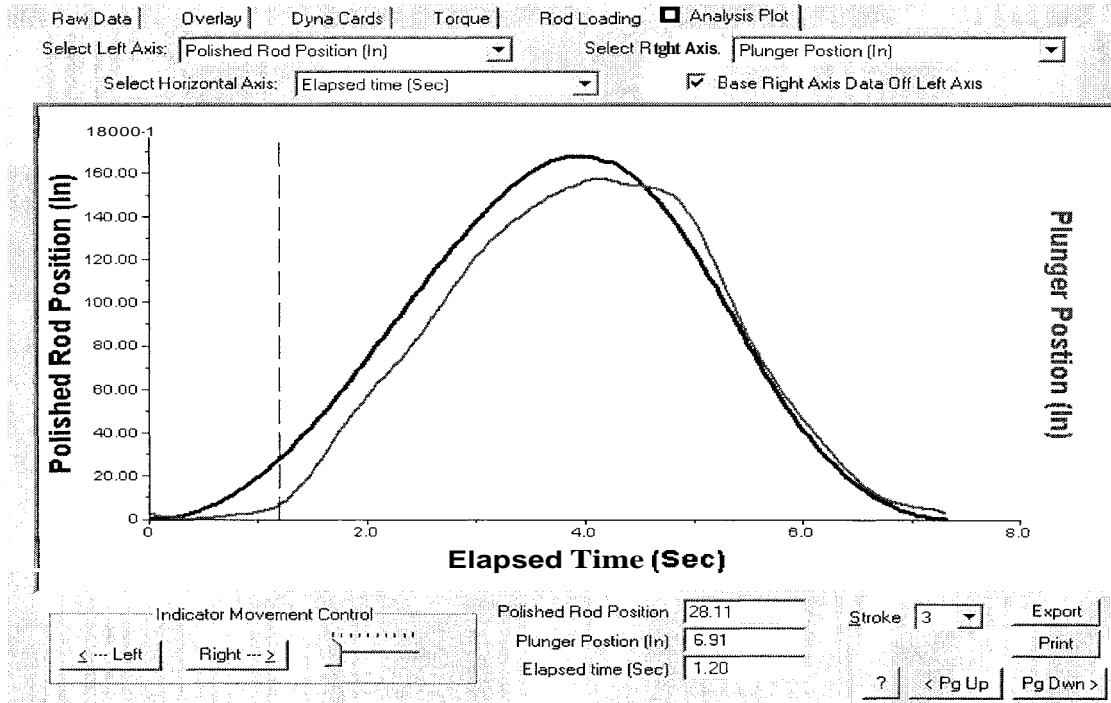


Figure 10 - Same as Figure 9 figure but TV Operating Normally with Full Pump

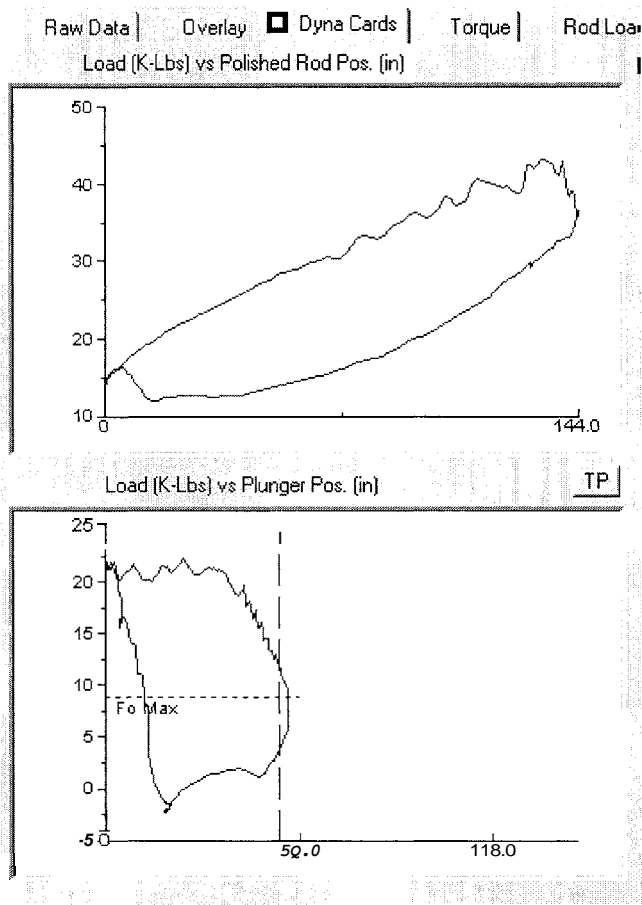


Figure 11 - Polished Rod and Plunger Dynamometer Cards for Well B

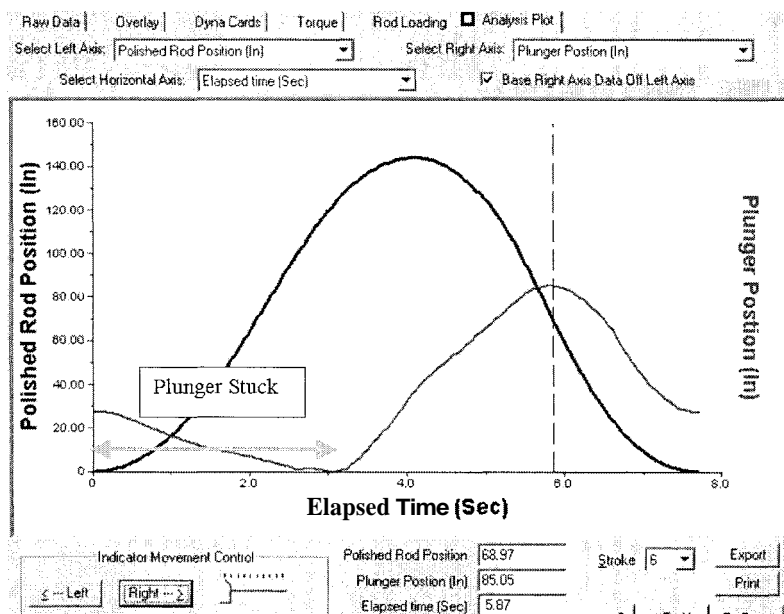


Figure 12 - Polished Rod and Plunger Position vs. Time for Well B (Stuck Plunger)

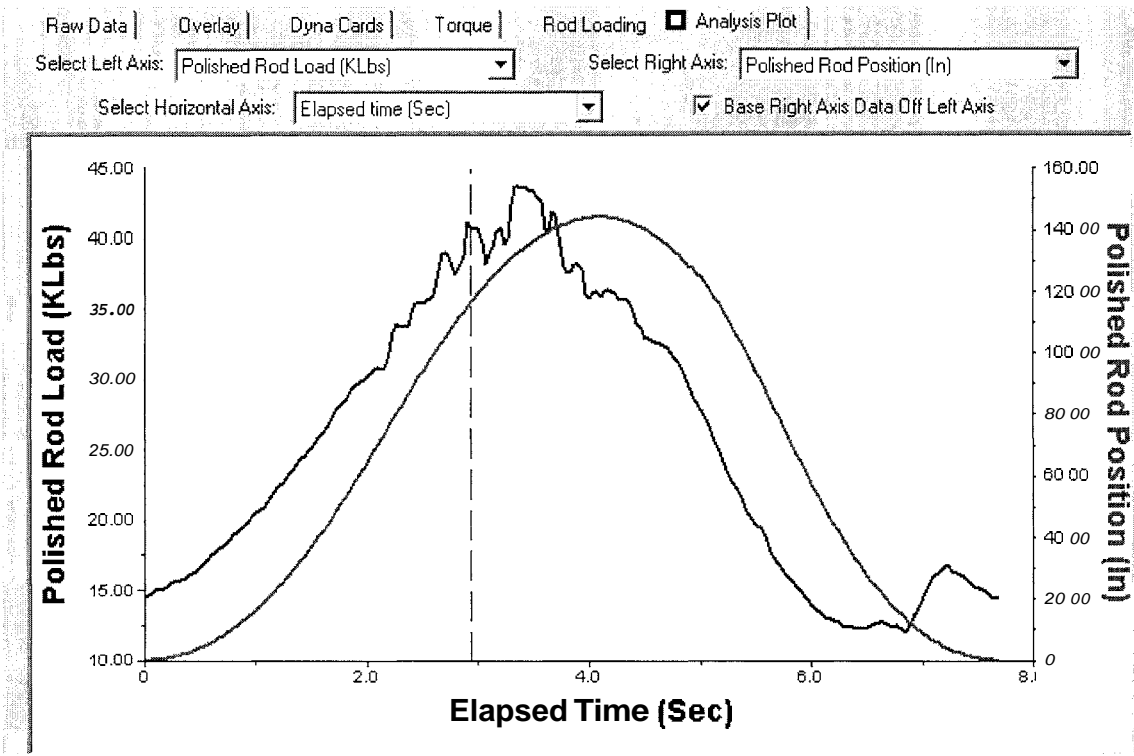


Figure 13 - Polished Rod Load and Position vs. Time for Well A (Stuck Plunger)

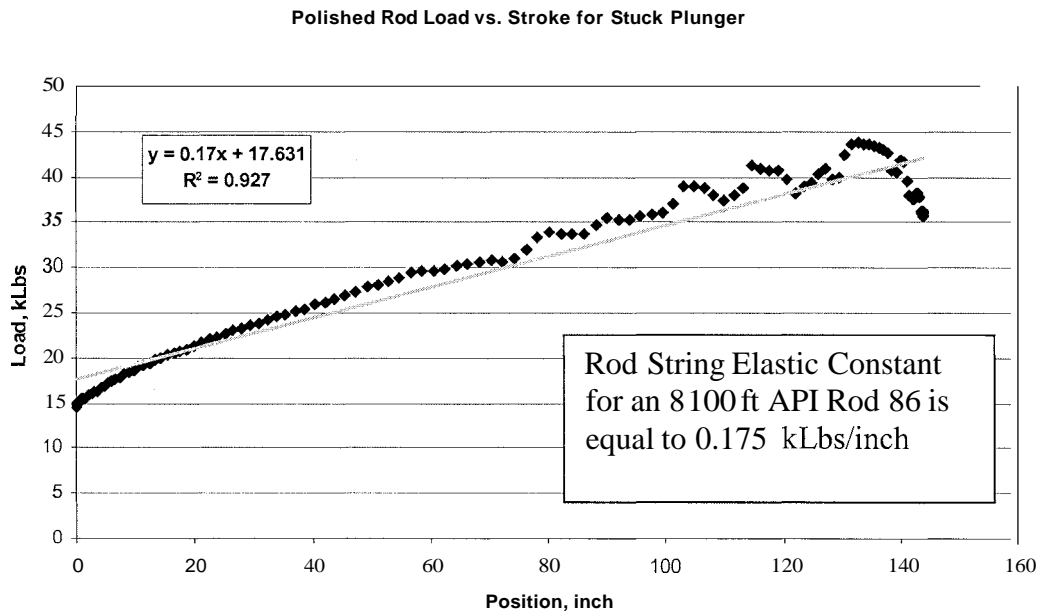


Figure 14 – Polished Rod Load vs. Polished Rod Position for Well A

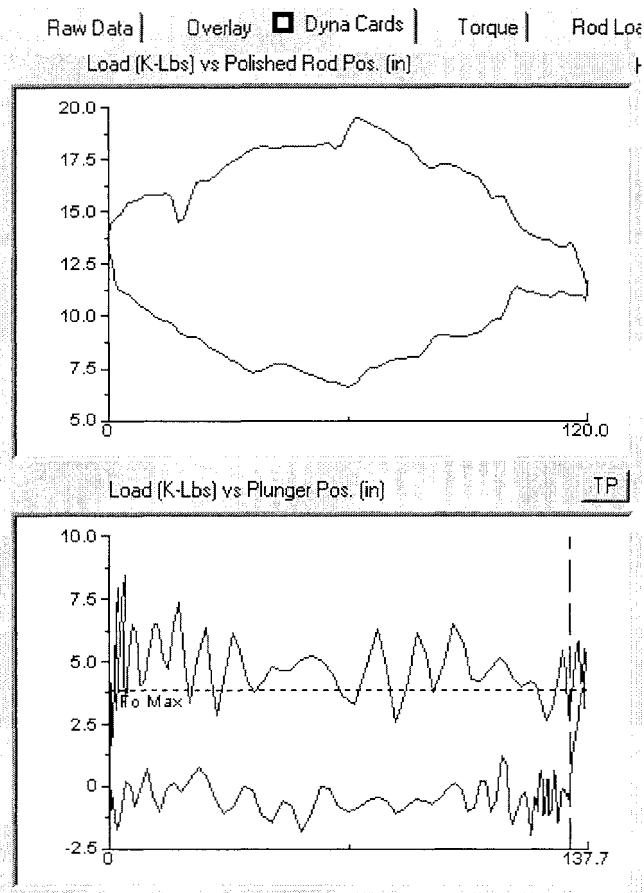


Figure 15 - Surface and Pump Dynamometer cards for Well C (Fiberglass Rods)

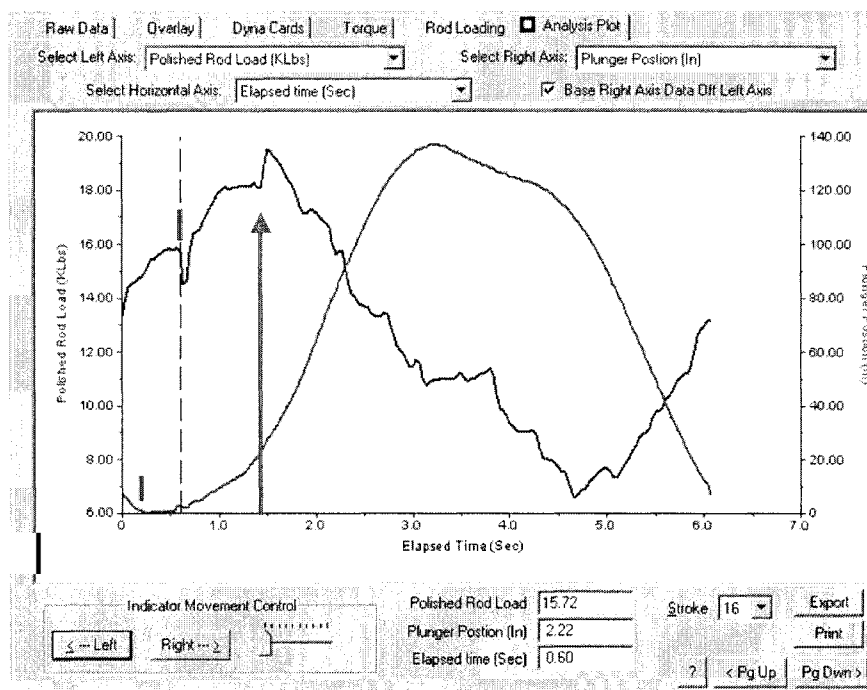


Figure 16 - Polished Rod Load and Plunger Position as a Function of Time for Well C

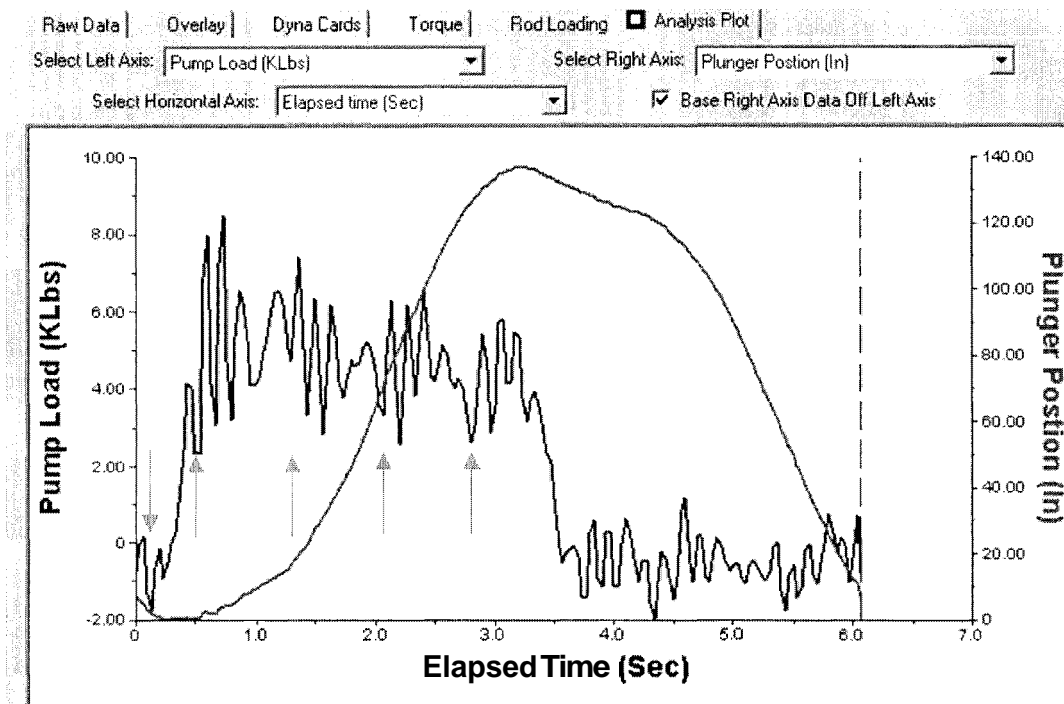


Figure 17 – Pump Load and Plunger Position vs. Time for Well C

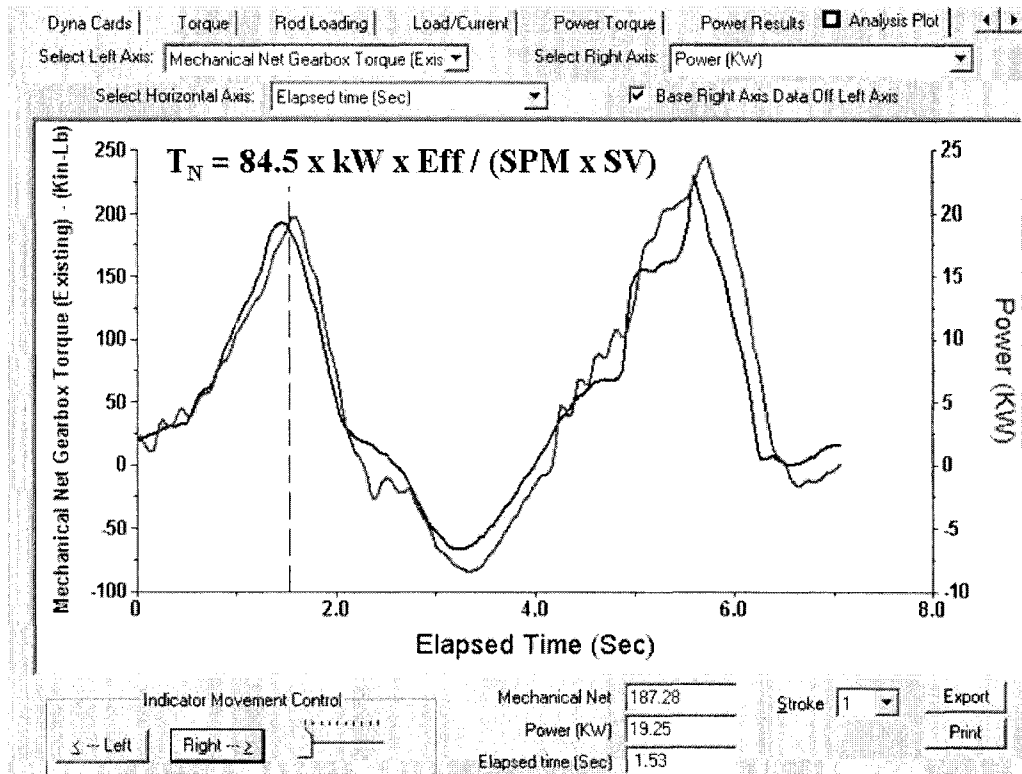


Figure 18 – Motor Input Motor Compared to Net Mechanical Gearbox Torque

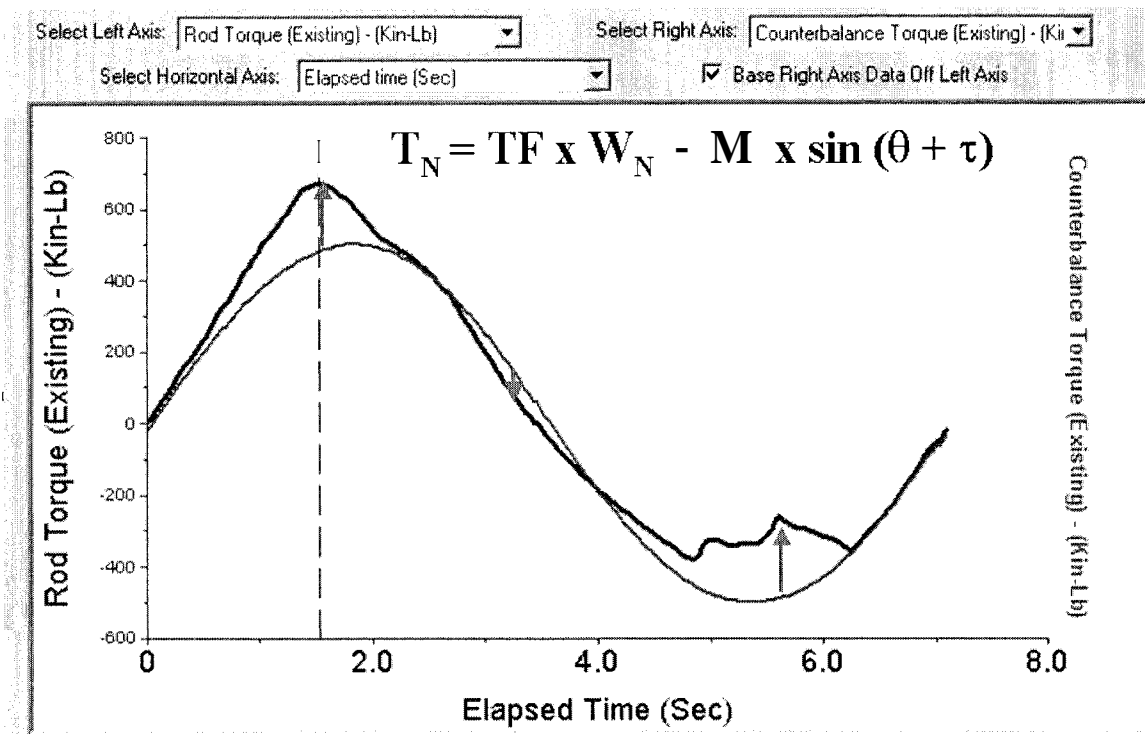


Figure 19 – Rod Torque Compared to Counterbalance Torque

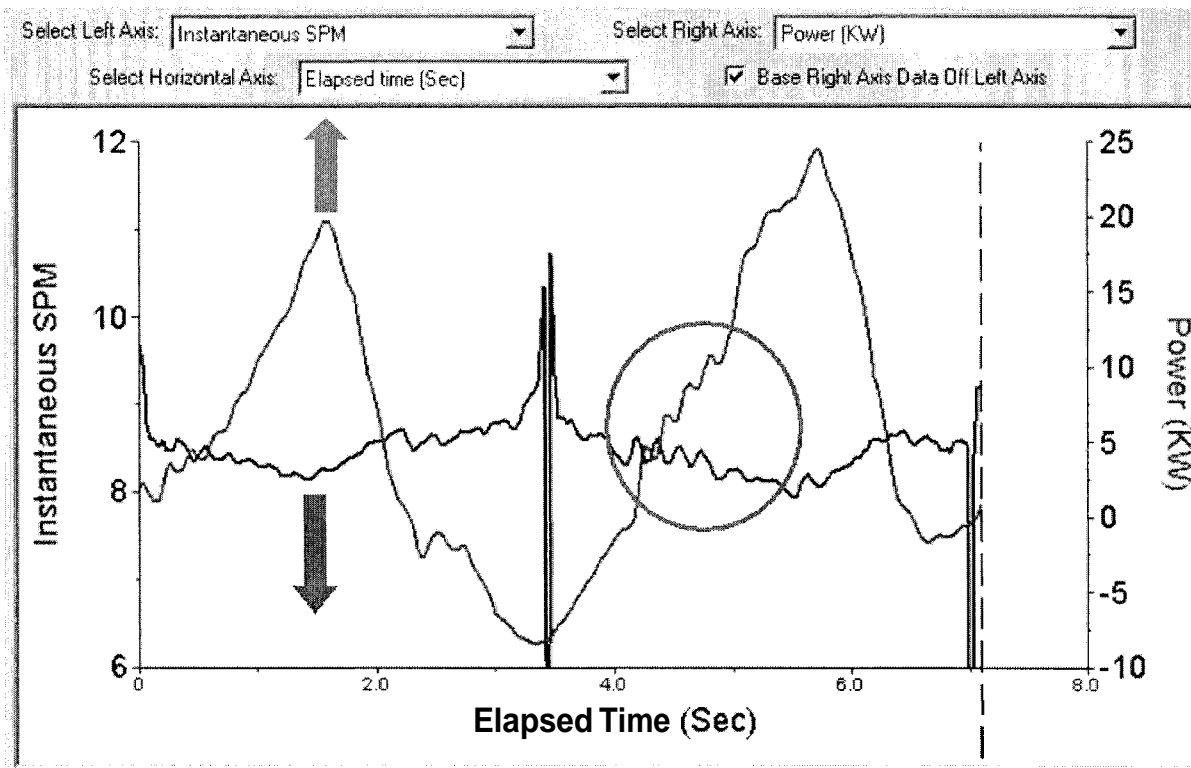


Figure 20 - Instantaneous Stroke per Minute in Comparison to Measured Input Motor Power

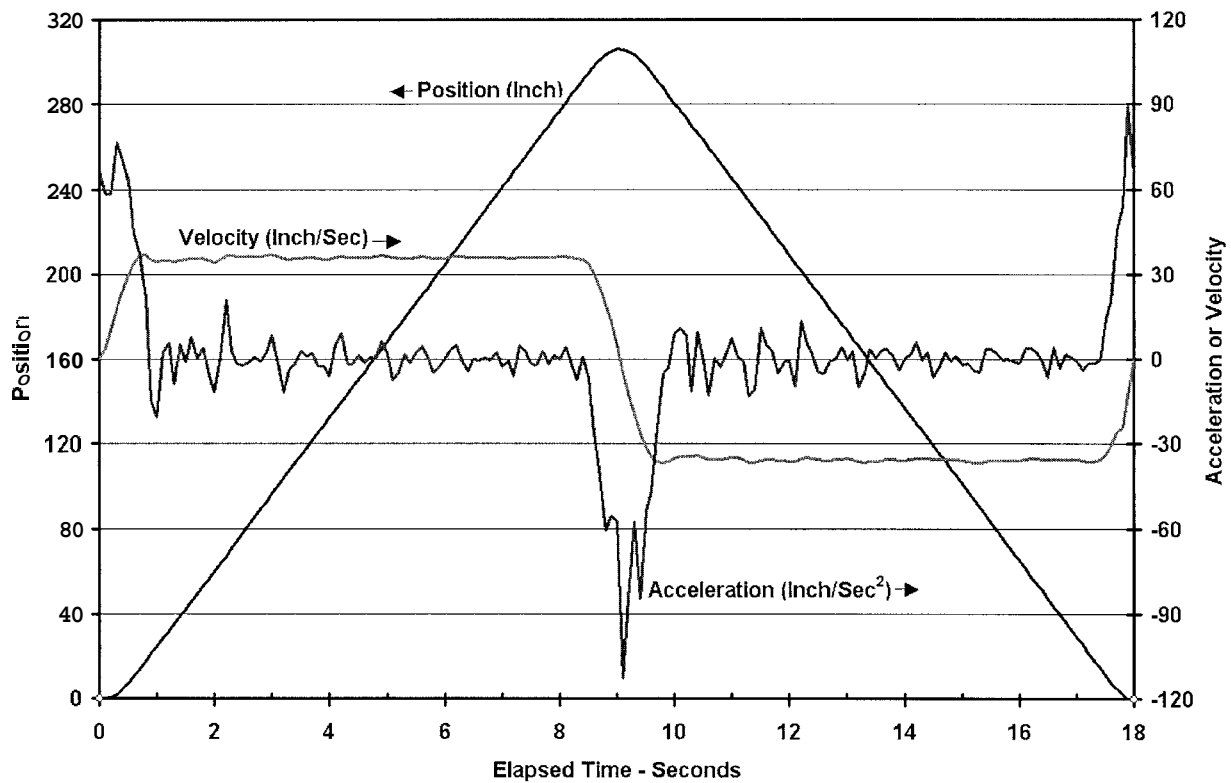


Figure 21 - Kinematics for RotaFlex Pumping Unit with Balanced Net Gearbox Torque

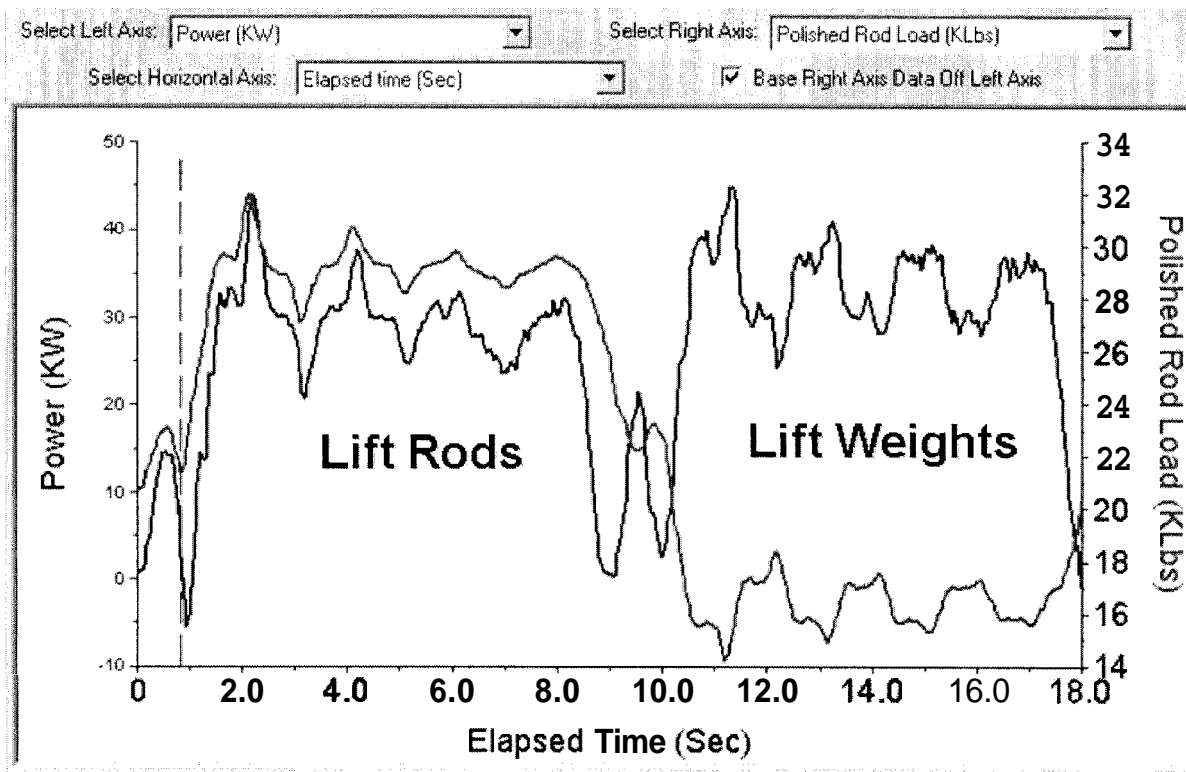


Figure 22 – RotaFlex Polished Rod Load Comparison to Measured Input Motor Power